Original Article

# Schisandrin B inhibits tumor progression of hepatocellular carcinoma by targeting the RhoA/ROCK1 pathway

**Hui Yang[1], Tengfei Wu[2]^**

[1]OBiO Technology (Shanghai) Corp., Ltd., Shanghai, China; [2]Department of Laboratory Animal Science, China Medical University, Shenyang, China

*Contributions:* (I) Conception and design: Both authors; (II) Administrative support: T Wu; (III) Provision of study materials or patients: H Yang; (IV) Collection and assembly of data: H Yang; (V) Data analysis and interpretation: Both authors; (VI) Manuscript writing: Both authors; (VII) Final approval of manuscript: Both authors.

*Correspondence to:* Tengfei Wu. Department of Laboratory Animal Science, China Medical University, 77 Puhe Road, Shenyang 110122, China. Email: Tfwu@cmu.edu.cn.

**Background:** Schisandrin B (Sch. B) performs various pharmacological properties, including anticancer activities. However, the pharmacological mechanisms of Sch. B in hepatocellular carcinoma (HCC) are not fully elucidated. We investigated the impact and mechanism on progression in HCC, and to provide new experimental evidence for HCC treatment.

**Methods:** To determine the inhibitory effect of Sch. B on HCC *in vivo*, 32 Balb/c nude mice were used to prepare the tumor-bearing mice model by subcutaneously inoculating HCC cells (Huh-7). As tumor volume grew to 100 $mm^3$, mice were randomly divided into Saline (control group), 100 mg/kg Sch. B group (Sch. B-L), 200 mg/kg Sch. B group (Sch. B-M), and 400 mg/kg Sch. B group (Sch. B-H) (n=8). Saline or different concentration Sch. B was used to treat mice via gavage administration for 21 days. After mice were euthanized, tumor weight and volume were evaluated. Cell apoptosis was detected by TUNEL. Ki-67 and PCNA were detected by immunohistochemical staining. The RhoA and Rho-associated protein kinase 1 (ROCK1) were determined by western blot. *In vitro* experiment, Huh-7 cell were treated by Sch. B at 40, 30, 20, 10, 5, 1, and 0 μM to detect cell proliferation by Cell Counting Kit-8 (CCK-8). Huh-7 cells were divided as a control group, Sch. B group, and Sch. B + RhoA overexpression (Sch. B + RhoA) group. RhoA and ROCK1 were examined. The colony formation assay and flow cytometry were used to detect cell proliferation and apoptosis. The wound healing and Transwell assays were used for cell metastasis detection.

**Results:** Our results showed 100, 200 and 400 mg/kg Sch. B significantly reduced tumor weight and volume. And 200 and 400 mg/kg Sch. B increased apoptosis, and reduced Ki-67 and PCNA levels, inhibited the RhoA and ROCK1 *in vivo* ($P<0.05$). *In vitro* experiment, Sch. B inhibited Huh-7 cell proliferation at concentration more than 10 μM ($P<0.05$). Sch. B decreased cell duplication, promoted apoptosis and blocked migration and invasion of Huh-7 ($P<0.05$). Sch. B inhibited RhoA and ROCK1 level as compared with control group ($P<0.05$). RhoA overexpression reversed the effect of Sch. B ($P<0.05$).

**Conclusions:** Sch. B inhibits Huh-7 cells progression via RhoA/ROCK1 pathway. The results provide new evidence for the clinical treatment of HCC.

**Keywords:** Hepatocellular carcinoma (HCC); Schisandrin B; RhoA/ROCK1 signaling pathway; progression

Submitted Jan 13, 2023. Accepted for publication Apr 23, 2023. Published online Apr 29, 2023.
doi: 10.21037/jgo-23-87
**View this article at:** https://dx.doi.org/10.21037/jgo-23-87

^ ORCID: 0000-0001-6154-1255.

## Introduction

Hepatocellular carcinoma (HCC) has become one of the most frequently diagnosed forms of malignancy (1). HCC's overall rate ranks sixth of all cancers and second in terms of mortality. Although the targeted therapy, the immunotherapy, and interventional therapy have become major strategies for treating cancer, treatment efficiency in HCC remains pessimistic due to rapid growth, metastasis, and drug resistance of HCC cells, and unfortunately these treatment options have limited success in HCC (2). One such agent is 5-fluorouracil (5-Fu), which inhibits thymidylate synthase and has shown a response rate of around 10% in HCC treatment (3). Accordingly, developing novel nontoxic and potent modulators to treat HCC is an urgent problem to be solved.

Schisandrin B (Sch. B), a potent dibenzocyclooctadiene derivative extracted from the fruit of the traditional Chinese medicinal plant *Schisandra chinensis* (Turcz.), has been reported to have significant inhibitory effects on a variety of solid malignancies, including colon, cervical, and breast cancers (4-6). Recently, He *et al.* reported that Sch. B inhibits the duplication of gastric cancer cells and promotes *5-fluorouracil* (5-FU) drug sensitivity (7). Yan *et al.* found that Sch. B promotes docetacxel-induced inhibition of cervical cancer progression (5). Sch. B has also been shown to reduce neoplastic changes in osteosarcoma (8). However, there are fewer studies reporting on the suppression effect of Sch. B on HCC cells.

The RhoA/rho-associated protein kinase 1 (ROCK1) pathway has been found to participate in regulating duplication and metastasis in HCC cells (9). It has been suggested that targeting the RhoA/ROCK1 signaling pathway may be an effective strategy for inhibiting HCC and breast cancer progression (10,11). However, there is little reported in the existing literature about the role of Sch. B in regulating the RhoA/ROCK1 pathway.

Based on those researches, we propose a scientific hypothesis that Sch. B performs the therapeutic impact on HCC progression *in vivo* and *in vitro* in italic, which is related with the RhoA/ROCK signaling pathway. Our results have provided compelling experimental results for the development of Sch. B for HCC therapy. We present the following article in accordance with the ARRIVE reporting checklist (available at https://jgo.amegroups.com/article/view/10.21037/jgo-23-87/rc).

### Highlight box

**Key findings**

- Sch. B inhibits the progression of HCC through RhoA/ROCK1 pathway.

**What is known and what is new?**

- Sch. B performs significant inhibitory effects on a variety of solid malignancies, including colon, cervical, and breast cancers.
- Sch. B significantly suppresses hepatocellular carcinoma cell proliferation, metastasis and promotes cell apoptosis *in vivo* and *in vitro* via regulating RhoA/ROCK1 signaling pathway.

**What is the implication, and what should change now?**

- Our results have provided compelling experimental data for the development of Sch. B for HCC therapy.

## Methods

### *Animal grouping and Sch. B treatment*

Firstly, we evaluated the inhibitory role of Sch. B on HCC using tumor-bearing mice model, which is well-established animal model of cancer. A total of thirty-two, half female and half male, 4–6-week-old, Balb/c nude mice were obtained from Liaoning Changsheng Biotechnology Co. Mice were bred at an airconditioned animal facility of China Medical University with 22±1 ℃ temperature and 45%±5% relative humidity. The entire animal protocol was approved by the Institutional Animal Care and Use Committee of China Medical University (No. CMU2021633), in compliance with institutional guideline for the care and use of animals. Once the tumor volume grew to 100 $mm^3$, the mice were put into 4 groups of 8 mice each using a random number table: control (Con) group, low-dose Sch. B (Sch. B-L), medium-dose Sch. B (Sch. B-M), and high-dose Sch. B (Sch. B-H). Mice in the different groups were treated with either saline only, 100, 200, or 400 mg/kg/d of Sch. B solution respectively, by gavage daily for 21 days. Sch. B was purchased from Chengdu Pufei De Biotech Co., Ltd. Sch. B was dissolved in dimethyl sulfoxide (DMSO), then diluted in Phosphate Buffered Saline (PBS) at final concentration of 5 mg/mL, 10 mg/mL and 20 mg/mL. After the final drug treatment, the mice were euthanized, and tumors were collected, weighed, and stored appropriately for subsequent experiments. A protocol was measured and prepared before the study without registration.

 

### *Terminal deoxynucleotidyl transferase dUTP nick-end labeling (TUNEL) experiment*

TUNEL assay was used to examine cell apoptosis. Formalin-fixed, paraffin-embedded tissues were sectioned at 4 μm thick using a microtome (Leica Biosystems RM2245 Microtome). Paraffin sections were prepared of the tumor tissues, and a TUNEL kit (Dalian Meilun Biotech, Dalian, China) was used to determine tumor tissue apoptosis. TUNEL procedures were carried out strictly according to the kit instructions. The tumor tissue was placed in an inverted fluorescent microscope (TE2000U, Nikon, Tokyo, Japan) to observe and count apoptotic cells.

### *Immunohistochemical staining (IHC)*

Ki-67 and proliferating cell nuclear antigen (PCNA) was determined for evaluating cell proliferation. Paraffin sections were used for detection of Ki-67 and PCNA levels. After hydration, antigen repair, and permeabilization, Ki-67 antibody (#34330,1:300, CST Biological Reagents Co., Ltd., Shanghai, China) or PCNA antibody (#13110, 1:300, CST) was added dropwise on the tissue surface and incubated overnight at 4 ℃. The Ki-67 or PCNA positive cells were observed under a microscope (BX53M, Olympus, Tokyo, Japan) and the positive rate was calculated.

### *Cell culture*

Human hepatocellular carcinoma cell line Huh-7 was obtained from American Type Culture Collection (ATCC, Rockville, MD, USA) and cultivated in Roswell Park Memorial Institute (RPMI)-1640 with 10% fetal bovine serum (FBS) and 1% penicillin-streptomycin in a 37 ℃ incubator. The RhoA overexpression plasmid was synthesized by Genepharma (Shanghai, China). After Huh-7 cells were cultured, Lipofectamine 3000 (Invitrogen, Carlsbad, CA, USA) was used to perform cell transfection according to the instructions.

### *Drug concentration selection and grouping*

Huh-7 cells were digested in 0.25% trypsin, then centrifuged at 1,500 rpm/min for 3 minutes, resuspended in fresh medium, adjusted to a concentration of $1.5\times10^5$/mL, and inoculated in 96-well plates with 100 μL each. Next, 100 μL of medium containing different dosages of Sch. B at final concentrations of 40, 30, 20, 10, 5, 1, and 0 μM was added to each well. The cells were then incubated for 24 hours, after which Cell Counting Kit-8 (CCK-8) staining solution was added. The Huh-7 cells were then further cultured for 120 minutes. The absorbance was determined according to the protocol. Cell survival rate (%) = ($A_{Sch.\ B}/A_{Con}$) ×100%.

For the subsequent experiment, Huh-7 cells were put into the following groups: control, Sch. B, RhoA overexpression, and Sch. B + RhoA overexpression. The cells in the control group were transfected with vector solution. The cells in the RhoA overexpression group were transfected with RhoA overexpression virus solution for 48 hours. The Sch. B and Sch. B + RhoA groups were treated with 10 μM Sch. B for 24 hours.

### *Colony formation assay*

Colony formation assay was performed to detect cell proliferation. Cells were digested and resuspended after 24 hours of Sch. B treatment, after which 500 cells/well were inoculated in 6-well plates and cultured for 14 days. The cells were then fixed in paraformaldehyde solution, followed by the addition of 1 mL of 0.1% crystalline violet staining solution and staining for 30 minutes. Cells were photographed using a digital camera, and the number of cell colonies was statistically analyzed.

### *Apoptosis examination*

After digestion by ethylenediaminetetraacetic acid (EDTA)-free trypsin following 24 hours of drug treatment, Huh-7 cells were centrifuged at 1,500 rpm/min for 3 minutes. Apoptosis was assessed using an FITC Annexin V/PI Apoptosis Detection Kit, and the apoptosis rate was calculated.

### *Scratch wound healing assay*

Scratch wound healing assay was used to examine cell migratory ability. HCC cells were cultivated and prepared as $1\times10^5$/mL cell suspension and spread in 6-well plates at 2 mL/well. Once 80% of cells were fused, the cell surface was scored with a pipette tip. Cells on the plate were then photographed by a light microscope (Olympus) at 0 hours and 24 hours after drug administration, and the migration rate was determined. Wound healing rate (%) = (1–scratch area/original scratch area) × 100%.

 

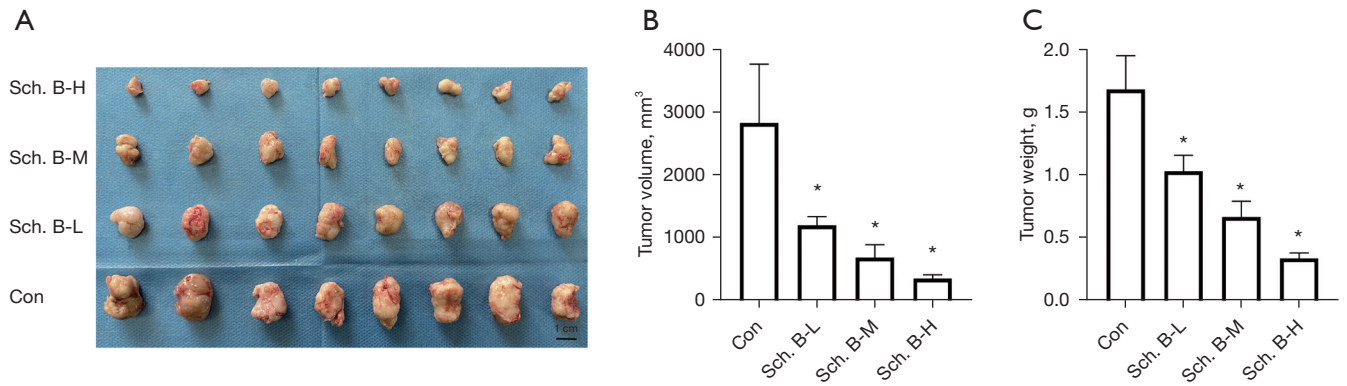


**Figure 1** The weight and volume of tumor in each group. (A) Representative pictures of tumors. (B) Tumor volume data (n=8). (C) Tumor weight results (n=8). *P<0.05 *vs.* Con group.

### *Transwell assay*

Transwell assay was used to examine cell invasion rate. Matrigel matrix gel and RPMI 1640-free medium were diluted 1:8 on ice and 50 μL Matrigel matrix gel was aliquoted to the upper chamber of the Transwell insert. Huh-7 cells were aliquoted to the upper layer at $4\times10^4$/well, followed by the addition of medium with FBS into the lower layer. After 48 hours cultivation, the Transwell chamber was removed, 4% paraformaldehyde was used for incubation for 15 minutes, and crystal violet solution was used to stain the cells for 30–40 minutes. Cells were then imaged by a light microscope (Olympus), and the cell invasion rate was calculated.

### *Western blot assay*

RhoA and ROCK1 levels were examined by western blot. Tumor tissues or Huh-7 cells were used for western blot. Whole proteins were purified using a protein extraction kit (Promega, Beijing, China). After quantified, 30 μg whole protein was loaded on sodium dodecyl by BCA method sulphate-polyacrylamide gel electrophoresis (SDS-PAGE) gel, transferred onto a polyvinylidene difluoride (PVDF) membrane, and then blocked at skim milk solution. Anti-RhoA (ab187027, Abcam) and anti-ROCK1 (ab134181, Abcam) antibodies were added and incubated overnight at 4 ℃. Diluted secondary antibodies (1:1,000, Abcam) were aliquoted and incubated for 2 hours. After detection by enhanced chemiluminescence (ECL) luminescence kit (Thermo Fisher Scientific, Madison, WI, USA), the protein blots were imaged in a gel imager and photographed. The grey scale values were calculated by Image J software [National Institutes of Health (NIH) image software].

### *Statistical analysis*

Measurements are showed as mean ± standard deviation (mean ± SD). Statistical analysis was performed by SPSS 21.0. Students *t* test was used for two-group comparisons. One-way analysis of variance (ANOVA) was performed for multiple comparison, and the least significant difference (LSD) test was used for two-way comparisons. P<0.05 was considered statistically significant.

## Results

### *Sch. B inhibits tumor weight and volume in HCC tumor-bearing mice*

We firstly explored the effect of Sch. B on HCC. HCC tumor-bearing mice were prepared and treated with different doses of Sch. B. As demonstrated in *Figure 1A,1B*, tumor volume in the Sch. B-L, Sch. B-M and Sch. B-H group were statistically reduced compared with that of control group (P<0.05). Moreover, as showed in *Figure 1C*, tumor weight in the Sch. B-L, Sch. B-M and Sch. B-H group were also remarkably decreased compared with that of control group (P<0.05).

### *Sch. B promotes cell apoptosis of HCC*

Cell apoptosis of tumor tissue under Sch. B treatment was detected by TUNEL assay (*Figure 2A*). There was no significant difference in apoptotic cells between the Sch. B-L and Con groups (P>0.05). Interestingly, there were

 

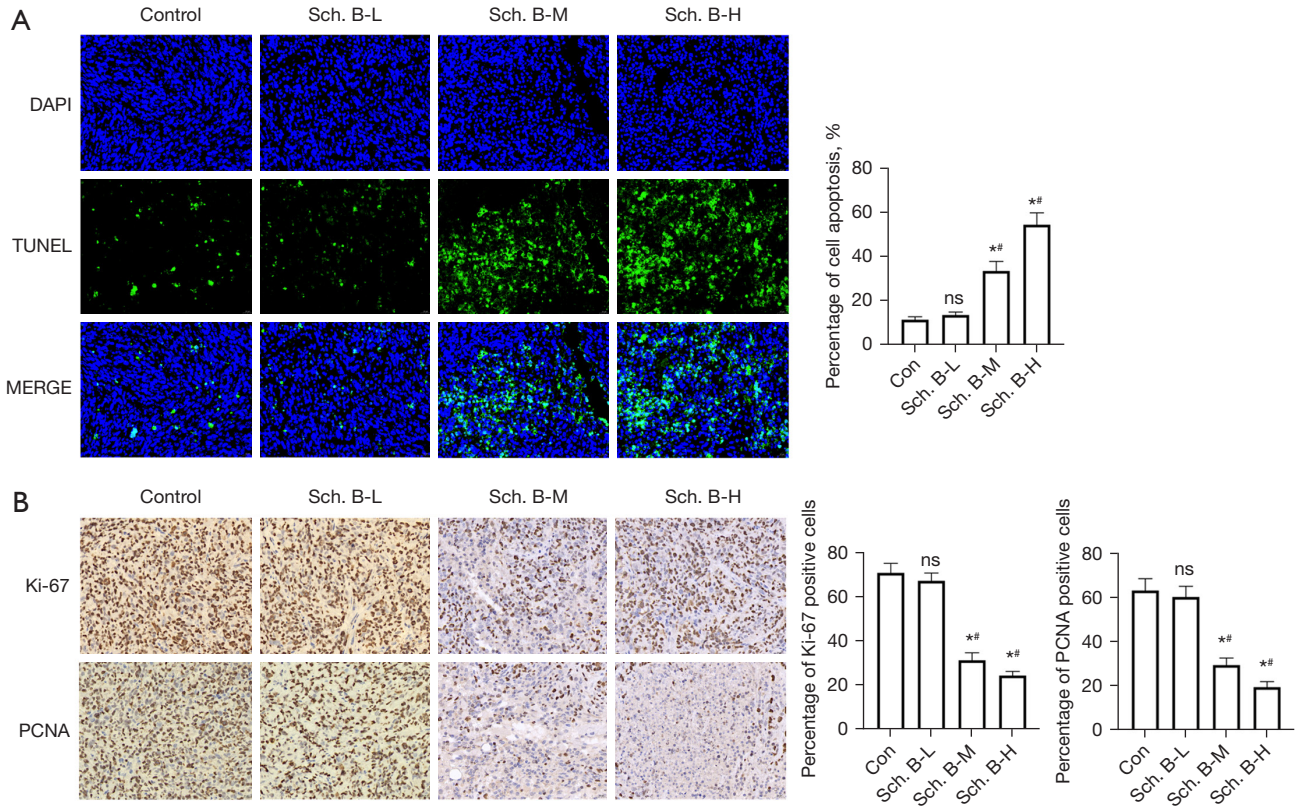


**Figure 2** Apoptotic cells in tumor tissue and the percentage of Ki-67 or PCNA positive cells in tumor tissues of tumor-bearing mice. (A) Apoptotic cells in tumor-bearing mice stained by DAPI marked by blue staining and TUNEL marked by green staining (n=3). Magnification, ×400. (B) Ki-67 or PCNA positive cells stained by IHC (%) (n=3). Magnification, ×400. *, P<0.05 *vs.* Con group. ns, P>0.05 *vs.* Con group. #, P<0.05 *vs.* Sch. B-L group. PCNA, proliferating cell nuclear antigen; IHC, immunohistochemical staining; TUNEL, Terminal deoxynucleotidyl transferase dUTP nick-end labeling; DAPI, 4',6-diamidino-2-phenylindole.

markedly more apoptotic cells in the Sch. B-M group and Sch. B-H group than that in the Con group (P<0.05).

### *Sch. B inhibits HCC cell duplication in mice tumor models*

To examine the regulatory role of Sch. B on HCC duplication, Ki-67 or PCNA expression in tumor tissue of Huh-7 xenograft mice were examined by IHC. As shown in *Figure 2B*, there was no significant difference in Ki-67 and PCNA positive cells in the Sch. B-L group (P>0.05). Interestingly, the number of Ki-67 and PCNA positive cells in tumor tissue of the Sch. B-M and Sch. B-L groups was less than that in Con group.

### *Sch. B blocks the RhoA/ROCK1 pathway in tumor tissues*

To further uncover the regulatory mechanism of Sch. B on the RhoA/ROCK1 pathway, RhoA and ROCK1 expression levels were determined by western blot. As shown in *Figure 3*, the expression of RhoA and ROCK1 in the tumor tissues of the Sch. B-L group was not significant (P>0.05). However, RhoA and ROCK1 expression in the Sch. B-M and Sch. B-H groups was significantly reduced (P<0.05). The above results indicated Sch. B promoted cell apoptosis and inhibited proliferation of tumor cells in tumor-bearing mice, which may have been related to inhibition of the RhoA/ROCK1 pathway.

### *The inhibitory effect of different Sch. B concentrations on HUH-7 cells*

After HUH-7 cells were incubated in different concentrations of Sch. B for 24 hours, the results of the CCK-8 assay showed that cell survival rate was decreased

 

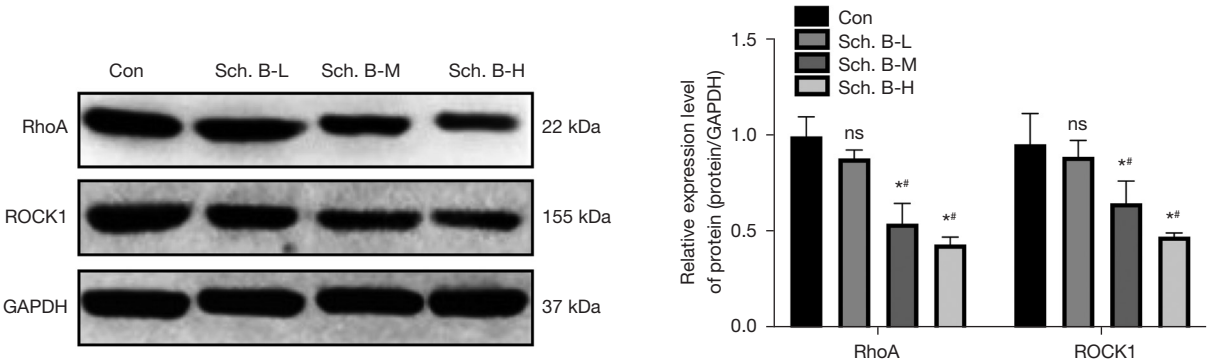


**Figure 3** Levels of RhoA and ROCK1 expression in tumor tissues under Sch. B treatment (n=3). *P<0.05 *vs.* Con group; #P<0.05 *vs.* Sch. B-L group; ns, P>0.05 *vs.* Con group.

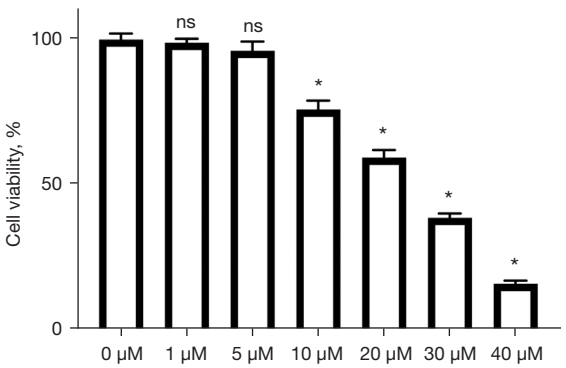


**Figure 4** CCK-8 results of Huh-7 cells with different amounts of Sch. B treatment (n=3). *P<0.05 *vs.* 0 μM group; ns, no significant. CCK-8, Cell Counting Kit-8.

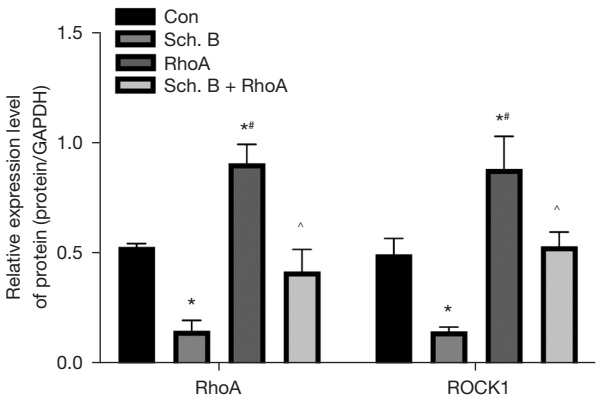


**Figure 5** The levels of RhoA and ROCK1 in Huh-7 cells (n=3). The final concentration of Sch. B is 10 μM. *, P<0.05 *vs.* Con group; #, P<0.05 *vs.* Sch. B group; ^, P<0.05 *vs.* RhoA group.

significantly (*Figure 4*). Cell viability under 1 and 5 μM Sch. B treatment was not significantly different compared with 0 μM Sch. B treatment (P>0.05). However, cell viability in the 10 μM, 20 μM, 30 μM, and 40 μM Sch. B groups was significantly lower than in the non-Sch. B treatment group (P<0.05). Therefore, 10 μM was chosen as the experimental concentration for subsequent experiments.

### *Sch. B regulates the RhoA/ROCK1 signaling pathway in Huh-7*

To further uncover the detailed mechanism of Sch. B on Huh-7 cells, RhoA overexpression cells were constructed to upregulate intracellular RhoA and ROCK1 levels. As shown in *Figure 5*, Sch. B markedly reduced RhoA and ROCK1 levels *in vitro* (P<0.05). Moreover, overexpression of RhoA could induce the expression of ROCK1 in Huh-7 (P<0.05).

### *Sch. B affects the proliferative capacity of Huh-7 cells through the RhoA/ROCK1 pathway*

*Figure 6* shows the number of cell colonies in the Sch. B group was significantly reduced (P<0.05). However, colony formation results also demonstrated that cell colonies in the Sch. B + RhoA group were remarkably increased compared with Sch. B treatment (P<0.05).

### *Sch. B promotes Huh-7 apoptosis via the RhoA/ROCK1 pathway*

The flow cytometry data are shown in *Figure 7*. These data demonstrated Sch. B treatment markedly promoted the apoptosis of Huh-7 cells (P<0.05). Interestingly, RhoA overexpression could partially block apoptosis induction

 

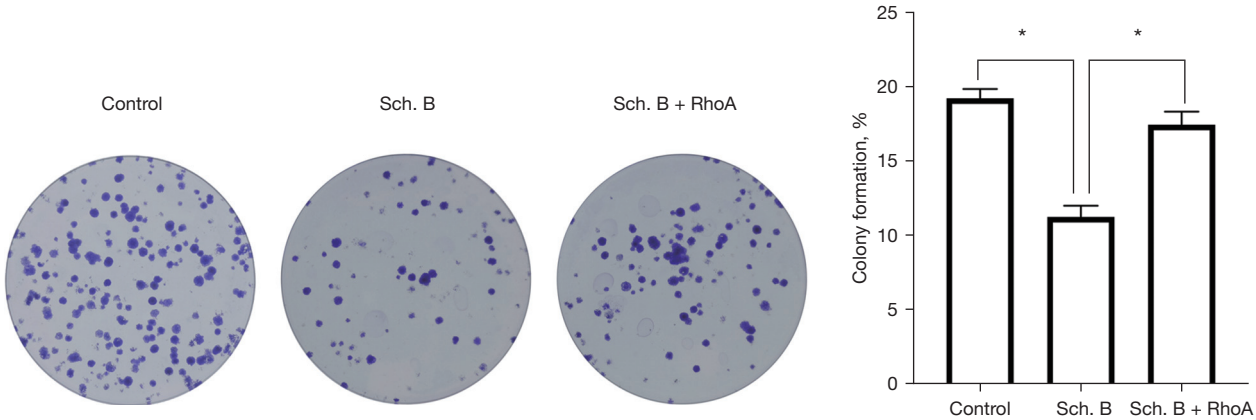


**Figure 6** Colony formation results of Huh-7 cells in each group stained by 0.1% crystalline violet staining (n=3). *P<0.05. The final concentration of Sch. B is 10 μM.

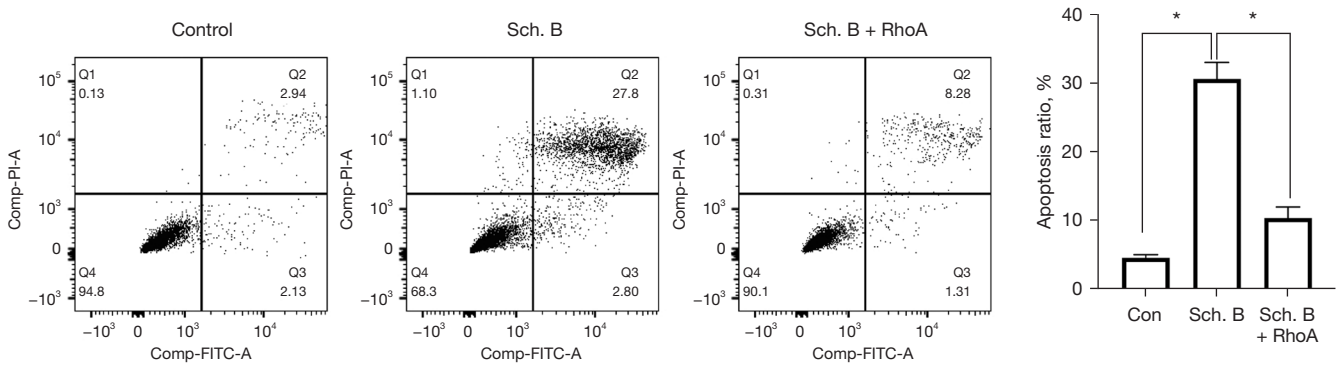


**Figure 7** Flow cytometry results of Huh-7 (n=3). *P<0.05. The final concentration of Sch. B is 10 μM. PI, propidium iodide staining; FITC, annexin V-FITC staining.

under Sch. B treatment (P<0.05). These data also indicated that Sch. B increased HUH-7 cell apoptosis dependance on the inhibition of RhoA.

### *Sch. B inhibits the metastasis of Huh-7 cells via the RhoA/ROCK1 pathway*

We also evaluated the impact of Sch. B on migration and invasion capability of HCC cells. *Figure 8A* shows Sch. B significantly reduced Huh-7 cell migration capability (P<0.05). Interestingly, the cell migration rate of the Sch. B + RhoA overexpression group was reversed than that the inhibitory effect in Sch. B treatment (P<0.05). In addition, the Transwell assay results (*Figure 8B*) show Huh-7 cell invasion under Sch. B treatment was significantly reduced (P<0.05). The invasion capability in the Sch. B + RhoA group was significantly higher than that in Sch. B treatment group (P<0.05).

## Discussion

Used for thousands of years to treat pandemics and endemic diseases, traditional Chinese medicine (TCM) is widely considered as the jewel of the nation (12). Sch. B is an active monomeric component of TCM that demonstrates antitumor activity (13). Liu *et al.* found Sch. B performed an inhibitory role in gastric cancer (14). He *et al.* reported that Sch. B increased the efficacy of chemotherapy drug 5-FU in gastric cancer cell (7). In addition, Sch. B has been shown to inhibit epithelial-mesenchymal transition and

 

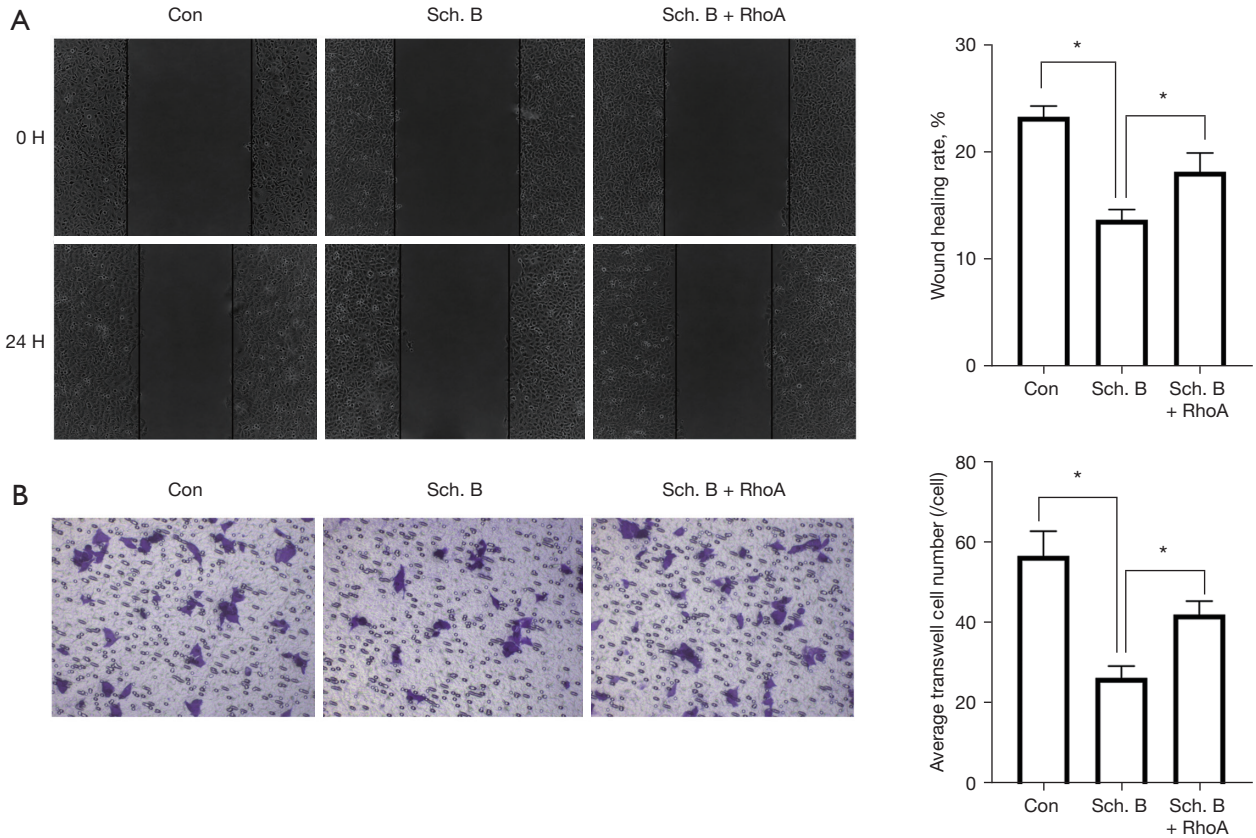


**Figure 8** The metastasis capability of Huh-7 under Sch. B treatment. (A) The results of scratch wound healing rate assay experiments (n=3). Cells were photographed by a light microscope (Olympus) at 0 hours and 24 hours after drug administration. Magnification, ×400. (B) The results of Transwell assay experiments stained by crystal violet solution (n=3). Cells were imaged by a light microscope (Olympus). Magnification, ×400; *P<0.05.

stemness in lung cancer by regulating the NF-κB and p38 MAPK pathways, thereby exerting an inhibitory effect (15). Sch. B has also been reported to block the Wnt-β-catenin and PI3K-Akt pathways to inhibit progression in osteosarcoma cells together with inducing apoptosis (8). Furthermore, in prostate cancer cells, Sch. B promotes cell apoptosis and oxidative stress as an effective agent for cancer therapy (16). Dai *et al.* found that Sch. B was effective for inhibiting triple negative breast cancer through regulation of STAT3 (6). Jiang *et al.* demonstrated that Sch. B could block the progression of glioma cells by regulating the HOTAIR–micoRNA-125a–mTOR axis (17). In our research, the therapeutic role of Sch. B was demonstrated by constructing mice xenograft models with Huh-7 cells. Our data demonstrated that tumor weight and volume in tumor-bearing mice were markedly reduced, cell numbers were markedly reduced, and the apoptotic index was also promoted under Sch. B treatment, indicating that Sch. B performed a promising anticancer role.

The RhoA/ROCK1 pathway is one of most important pathways in tumor cell motility and morphogenesis, which is associated with cell metastasis (18,19). RhoA belongs to the Rho family of GTPases, which contributes to F-actin polymerization forming stress fibers to regulate actin movement and cellular contractility. In addition, the activation of ROCK1 by RhoA has been shown to promote the formation of local adhesion of tumor cells, thus allowing their movement, with the result that the RhoA/ROCK1 signaling pathway affects tumor cell migration and invasion (10,19). During tumor cell migration and

 

invasion, cell adhesion capacity, cytoskeletal alterations, and the polarization of cells are associated with a stimulated RhoA/ROCK1 pathway. Many studies have shown that over activating the RhoA/ROCK1 pathway in HCC could induce migration and invasion ability (10,20). Similar results were reported in breast and gastric cancer cells, where the stimulation of the RhoA/ROCK1 signaling pathway was found to promote cell migration (21,22). Therefore, the inhibition of RhoA/ROCK1 signaling pathway activity is considered an effective way to inhibit HCC progression.

Our data demonstrated RhoA and ROCK1 expression levels were promoted in tumor tissues of mice, indicating the RhoA/ROCK1 pathway was markedly activated, which is consistent with the results of a previous study (9). After Sch. B treatment, RhoA and ROCK1 levels in tumor tissues were significantly reduced, suggesting Sch. B treatment in liver cancer could be related to inactivation of the RhoA/ROCK1 pathway. You *et al.* investigated that Schisandrin A inhibit the RhoA/ROCK1 pathway to promote pulmonary capillary endothelial (23). Other study found that Schisandrin A recovered erectile dysfunction through regulating RhoA/ROCK1 pathway in type 1 diabetes mice (24). However, the regulatory role of Sch. B on RhoA/ROCK1 pathway was not reported. To further verify the detailed molecular mechanism of Sch. B treatment in HCC, we constructed Huh-7 cells overexpressing RhoA *in vitro*. Our data demonstrated that RhoA and ROCK1 levels were markedly increased in Huh-7 cells after transfection with RhoA overexpression viral-based vector, indicating that the RhoA/ROCK1 signaling pathway was markedly activated. After Sch. B treatment, RhoA and ROCK1 levels were significantly reduced, which was consistent with the results *in vivo*. Interestingly, Sch. B could partially reverse the activation of RhoA/ROCK1 signaling pathway by overexpression of RhoA. In addition, the proliferation, migration, and invasion abilities under Sch. B treatment were significantly reduced, and apoptotic cells were also increased. These results suggested that Sch. B could partially reverse the impact of RhoA overexpression in HCC cell proliferation, apoptosis, migration, and invasion, indicating that Sch. B suppressed the proliferation and metastasis of HCC by downregulating the RhoA/ROCK1 pathway. There is a limitation that we did not examine other mechanisms in Sch. B regulating on HCC cell. And we will explore this in a follow-up study.

## Conclusions

Sch. B regulates the migratory, invasion, and proliferation processes of HCC by inhibiting the RhoA/ROCK1 signaling pathway. Our results have provided a new therapeutic approach for effectively slowing down the progression of HCC. However, the specific molecular mechanism needs to be further investigated and confirmed.

## Acknowledgments

*Funding:* None.

## Footnote

*Reporting Checklist:* The authors have completed the ARRIVE reporting checklist. Available at https://jgo.amegroups.com/article/view/10.21037/jgo-23-87/rc

*Data Sharing Statement:* Available at https://jgo.amegroups.com/article/view/10.21037/jgo-23-87/dss

*Peer Review File:* Available at https://jgo.amegroups.com/article/view/10.21037/jgo-23-87/prf

*Conflicts of Interest:* Both authors have completed the ICMJE uniform disclosure form (available at https://jgo.amegroups.com/article/view/10.21037/jgo-23-87/coif). HY is from OBiO Technology (Shanghai) Corp., Ltd. The other author has no conflicts of interest to declare.

*Ethical Statement:* The authors are accountable for all aspects of the work in ensuring that questions related to the accuracy or integrity of any part of the work are appropriately investigated and resolved. The entire animal protocol was approved by the Institutional Animal Care and Use Committee of China Medical University (No. CMU2021633), in compliance with institutional guideline for the care and use of animals.



 

## References


1. Xia C, Dong X, Li H, et al. Cancer statistics in China and United States, 2022: profiles, trends, and determinants. Chin Med J (Engl) 2022;135:584-90.
2. Sung H, Ferlay J, Siegel RL, et al. Global Cancer Statistics 2020: GLOBOCAN Estimates of Incidence and Mortality Worldwide for 36 Cancers in 185 Countries. CA Cancer J Clin 2021;71:209-49.
3. Lin DY, Lin SM, Liaw YF. Non-surgical treatment of hepatocellular carcinoma. J Gastroenterol Hepatol 1997;12:S319-28.
4. Pu Z, Zhang W, Wang M, et al. Schisandrin B Attenuates Colitis-Associated Colorectal Cancer through SIRT1 Linked SMURF2 Signaling. Am J Chin Med 2021;49:1773-89.
5. Yan C, Gao L, Qiu X, et al. Schisandrin B synergizes docetaxel-induced restriction of growth and invasion of cervical cancer cells in vitro and in vivo. Ann Transl Med 2020;8:1157.
6. Dai X, Yin C, Guo G, et al. Schisandrin B exhibits potent anticancer activity in triple negative breast cancer by inhibiting STAT3. Toxicol Appl Pharmacol 2018;358:110-9.
7. He L, Chen H, Qi Q, et al. Schisandrin B suppresses gastric cancer cell growth and enhances the efficacy of chemotherapy drug 5-FU in vitro and in vivo. Eur J Pharmacol 2022;920:174823.
8. Wang Y, Chen J, Huang Y, et al. Schisandrin B suppresses osteosarcoma lung metastasis in vivo by inhibiting the activation of the Wnt/β catenin and PI3K/Akt signaling pathways. Oncol Rep 2022;47:50.
9. Zhang JG, Zhou HM, Zhang X, et al. Hypoxic induction of vasculogenic mimicry in hepatocellular carcinoma: role of HIF-1 α, RhoA/ROCK and Rac1/PAK signaling. BMC Cancer 2020;20:32.
10. Lin L, Li M, Lin L, et al. FPPS mediates TGF-β1-induced non-small cell lung cancer cell invasion and the EMT process via the RhoA/Rock1 pathway. Biochem Biophys Res Commun 2018;496:536-41.
11. Matsubara M, Bissell MJ. Inhibitors of Rho kinase (ROCK) signaling revert the malignant phenotype of breast cancer cells in 3D context. Oncotarget 2016;7:31602-22.
12. Xu J, Zhang Y. Traditional Chinese Medicine treatment of COVID-19. Complement Ther Clin Pract 2020;39:101165.
13. Lv XJ, Zhao LJ, Hao YQ, et al. Schisandrin B inhibits the proliferation of human lung adenocarcinoma A549 cells by inducing cycle arrest and apoptosis. Int J Clin Exp Med 2015;8:6926-36.
14. Liu XN, Zhang CY, Jin XD, et al. Inhibitory effect of schisandrin B on gastric cancer cells in vitro. World J Gastroenterol 2007;13:6506-11.
15. Li S, Wang H, Ma R, et al. Schisandrin B inhibits epithelial mesenchymal transition and stemness of large cell lung cancer cells and tumorigenesis in xenografts via inhibiting the NF κB and p38 MAPK signaling pathways. Oncol Rep 2021;45:115.
16. Nasser MI, Han T, Adlat S, et al. Inhibitory effects of Schisandrin B on human prostate cancer cells. Oncol Rep 2019;41:677-85.
17. Jiang Y, Zhang Q, Bao J, et al. Schisandrin B inhibits the proliferation and invasion of glioma cells by regulating the HOTAIR-micoRNA-125a-mTOR pathway. Neuroreport 2017;28:93-100.
18. Yan L, Li H, An W, et al. Mex-3 RNA binding MEX3A promotes the proliferation and migration of breast cancer cells via regulating RhoA/ROCK1/LIMK1 signaling pathway. Bioengineered 2021;12:5850-8.
19. Ko E, Kim D, Min DW, et al. Nrf2 regulates cell motility through RhoA-ROCK1 signalling in non-small-cell lung cancer cells. Sci Rep 2021;11:1247.
20. Zhang K, Na T, Ge F, et al. DLC-1 tumor suppressor regulates CD105 expression on human non-small cell lung carcinoma cells through inhibiting TGF-β1 signaling. Exp Cell Res 2020;386:111732.
21. Gilkes DM, Xiang L, Lee SJ, et al. Hypoxia-inducible factors mediate coordinated RhoA-ROCK1 expression and signaling in breast cancer cells. Proc Natl Acad Sci U S A 2014;111:E384-93.
22. Yu SY, Peng H, Zhu Q, et al. Silencing the long noncoding RNA NORAD inhibits gastric cancer cell proliferation and invasion by the RhoA/ROCK1 pathway. Eur Rev Med Pharmacol Sci 2019;23:3760-70.
23. You LJ, Li PW, Zhang WW, et al. Schisandrin A ameliorates increased pulmonary capillary endothelial permeability accompanied with sepsis through inhibition of RhoA/ROCK1/MLC pathways. Int Immunopharmacol


 

2023;118:110124.
24. Hao H, Zhang R, Guo P, et al. Schisandrin A ameliorates erectile dysfunction and regulates RhoA/ROCK1 pathway in rats with streptozotocin-induced type 1 diabetes. Pharmacognosy Magazine 2022;18:766-72.

(English Language Editor: A. Muijlwijk)

**Cite this article as:** Yang H, Wu T. Schisandrin B inhibits tumor progression of hepatocellular carcinoma by targeting the RhoA/ROCK1 pathway. J Gastrointest Oncol 2023;14(2):533-543. doi: 10.21037/jgo-23-87

 